Journal of
Ceramic Science
and Technology

J. Ceram. Sci. Tech., **05** [02] 115-124 (2014)
DOI: 10.4416/JCST2013-00036
available online at: http://www.ceramic-science.com
© 2014 Göller Verlag

Low-Carbon Carbon-Bonded Alumina Refractories for Functional Components in Steel Technology

V. Stein[*1,2], **C. G. Aneziris**[1]

[1]Technische Universität Bergakademie Freiberg Institut für Keramik, Glas- und Baustofftechnik, Agricolastrasse 17, 09599 Freiberg, Germany
[2]Refratechnik Steel GmbH, Schiessstrasse 58, 40549 Düsseldorf, Germany
received November 3, 2013; received in revised form January 3, 2014; accepted February 5, 2014

Abstract

Carbon-bonded alumina refractories (Al_2O_3-C) are essential for modern steelmaking practice. The typical carbon content for functional materials is approximately 30 wt%. With regard to environmentally friendly refractory systems, this work has observed and described the interaction of functional silicon (n-type semiconductor) with an organic binder system. With this system, it was possible to lower the carbon content to 15 wt% without downgrading the material properties. On the contrary, the properties were improved. As a result of the upgrading of the microstructural flexibility and the mechanical strength, the thermal shock performance could be enhanced. The mechanism is based on electron transfer from the n-type semiconductor to the binder resite lattice. The result is a flexible, partially graphitized carbon bonding matrix. This aspect had been studied previously in a CaO-MgO-C system and is of great interest with regard to reduced emissions and environmentally friendly refractory materials.

Keywords: Alumina, graphite, electron transfer

I. Introduction

Carbon-bonded alumina refractories (Al_2O_3-C) are an essential part of modern steelmaking practice. Refractories of this group are widely used as functional components in continuous steel casting operations. For these applications, a carbon content of approximately 30 wt% is widely used.

Quintessential components are submerged entry nozzles, monobloc stoppers and ladle shrouds. To ensure occupational safety and effective productivity at the steel plant, these heavy-duty materials need to fulfil a number of essential and partially contrasting demands. The most important demands are high corrosion and erosion resistance, low wettability against steel and slag melts, high thermal shock performance, as well as high mechanical strength and oxidation resistance at elevated temperatures. The ongoing optimization of these properties is a necessary goal, especially in the context of environmental protection.

The two main components of the Al_2O_3-C system, namely alumina and carbon, exhibit very high refractoriness and excellent corrosion resistance. Alumina has very low free energy of formation, like CaO and MgO (Table 1). Al_2O_3 exhibits high mechanical strength as well as high corrosion and abrasion resistance. Graphite has very high refractoriness. Its sublimation point is about 4000 K at 1 atm [1]. Furthermore, graphite exhibits strong anisotropic behaviour.This is reflected in its thermal expansion ($\approx 10...50 \cdot 10^{-7}$ K^{-1}), thermal conductivity (≈ 80 W/mK), modulus of elasticity and mechanical strength. The high thermal conductivity and the low thermal expansion coefficient are responsible for its excellent thermal shock resistance. Graphite offers very good corrosion resistance against many inorganic as well as organic acids and salt solutions. In addition, it should be noted that graphite exhibits very low wettability by slags and molten metals [2,3]. In combination with Al_2O_3, it improves the slagging resistance and increases the elasticity of the composite material. Furthermore, it decreases the cold modulus of rupture (CMOR) as well as the bulk density of the composite. A big disadvantage of graphite is its high susceptibility to oxidation [4,5,6,7].

Table 1: Free enthalpies of formation of common refractory oxides at 1800 K and 101325 Pa[8].

		ΔG_{1800K} in kj/mol
$2Ca+O_2 \rightarrow 2CAO$	(1)	-886,87
$\frac{4}{3}Al+O_2 \rightarrow \frac{2}{3}Al_2O_3$	(2)	-738,21
$2Mg+O_2 \rightarrow 2MgO$	(3)	-726,57
$Si+O_2 \rightarrow SiO_2$	(4)	-590,98
$\frac{4}{3}Cr+O_2 \rightarrow \frac{2}{3}Cr_2O_3$	(5)	-441,97

* Corresponding author: Volker.Stein@refra.com

The combination of alumina and graphite yields a material with high performance with regard to thermal shock resistance, corrosion resistance and mechanical strength.

The third essential component of this refractory material group is the organic binder. A common bonding medium in carbon-bonded refractories are artificial phenolic resins. The binder is responsible for the adherence of the composite components. Phenolic resins are a common binder for carbon-bonded refractories. Novolak is one of two types of phenolic resins. Phenolic resins are condensation products of phenol and formaldehyde in an alkaline (resol) or acidic (novolak) catalytically driven process. Resol contains methylol groups (CH_2OH) while novolak is characterized by an absence of these methylol groups. These groups are necessary for the polymerization process of the phenolic resins to phenol plastics. For novolak resin, the addition of Hexamethylenetetramine (Hexa) is necessary to provide methylol groups [9].

The curing process (polymerization of the macromolecules) takes place at temperatures above 160 °C. Novolak is polymerized under the addition of Hexa at temperatures above 120 °C in two steps up to 170 °C with ammonia splitting off while methylene bridges are formed. Split-off formaldehyde also leads to an additional linking. The added Hexa is almost completely consumed at the beginning of the reaction. In the polymerization process (also called curing or hardening), a three-dimensional cross-linked lattice is formed. This lattice is known as a resite lattice. It is very hard, insoluble and unmeltable. An increasing Hexa content leads to better cross-linking of the resin and an increasing residual carbon content. Furthermore, the mechanical strength increases and the open porosity decreases [9].

Phenolic resins are solid at ambient temperature and standard pressure. The solid resin in pulverized form is used directly as binder. Furthermore, liquid resin is produced by dissolving the solid resin in an organic solvent. The residual carbon content of liquid resins lies below that of solid resins.

After polymerization the resite lattice transforms under reducing or inert conditions in a coking process (pyrolysis) up to 1000 °C into essentially elementary carbon and forms a carbon lattice, the so-called glassy carbon lattice. In the coking process the resite lattice is dehydrated and hydro carbons are split off, so volatile components diffuse out of the body into the atmosphere. Several complex reactions like dehydrogenation, condensation and isomerization take place at the same time. The glassy carbon lattice dominates the bonding of carbon-bonded refractories and is characteristic for the properties of carbon-bonded refractories. The problem of the glassy carbon lattice is the high susceptibility to oxidation owing to its large inner surface [1, 10, 11].

Glassy carbon has belt-like graphitic areas. In these areas the carbon atoms are sp^2 hybridized and are found in layers. These layers are interloop-disordered and no regular crystal order of the graphitic areas exists. They are stochastically ordered and have many vacancies. Owing to its structure, glassy carbon has a lower density than graphite and has isotropic low thermal and electrical conductivities, as well as high hardness. The material is exceedingly resistant to abrasion and chemicals. It can only be attacked by oxygen and oxidizing melts above 600 °C [1, 2, 12, 13, 14]. The glassy carbon lattice provides the bonding of carbon-bonded refractory systems. This structure can be graphitized with the aid of iron metals as well as nickel in a catalytically driven process [15, 16]. Furthermore, the structure can be partially graphitized with the aid of electron donating species, like TiO_2, ZrO_2 and n-Si [17, 18, 19]. Graphitization leads to a more flexible structure, which is able to withstand high mechanical stresses owing to higher breaking elongation.

Both process steps, polymerization and pyrolysis, release various emissions. So the production and application of carbon-bonded refractories is linked to environmentally harmful emissions in the broadest sense. Based on the Kyoto protocol and the German Federal Emission Control Act, it is a general aim to reduce emissions [20, 21]. It is necessary to keep in mind that carbon and specifically graphite is a necessary component in this refractory group. Reducing the graphite content also changes the properties. So it is important to keep the main properties level with the original values.

State of the art in combating the moderate oxidation resistance of Al_2O_3-C refractories is the use of antioxidants. A side-effect of their application is mechanical reinforcement. Antioxidants are typically fine metallic powders like silicon or aluminium up to a particle size of 150 μm. Carbides (SiC, B_4C, Al_4SiC_4, $Al_8B_4C_7$) and boron-containing oxides (fluxes) in the range up to a particle size of 100 μm are also used as antioxidants [22–29]. The improvement in the oxidation resistance is achieved with the following mechanisms: the antioxidant, for example metallic silicon, reacts with gaseous CO in the surrounding atmosphere, forming gaseous SiO and reducing gaseous CO to solid C, thus suppressing oxidation loss of carbon [23]. The formed gaseous SiO further reacts with gaseous CO and deposits a thin protective layer of solid SiO_2 on the graphite surface, thus reducing the active sites [27]. These reactions are accompanied by a volume expansion, which can seal the pores of the material [22, 23].

The present work is part of the Priority Program 1418 funded by the German Research Foundation (GRF) with the aim of reducing the carbon content of alumina carbon refractories without downgrading their properties. The results presented here are the second part in a wider field of observations following a new and innovative path. In the first step of the project it was possible to lower the carbon content from 30 to 20 wt% by adding nano-scaled additives to achieve better thermal shock performance [30, 31]. Mainly multi-walled carbon-nanotubes and alumina nano-sheets were used to provoke a beneficial formation of nano-scaled structures that worked as connecting elements between the carbon lattice and oxide grains.The newly found Al_3CON phase was predominantly responsible for the mechanical reinforcement of the Al_2O_3-C refractory. Besides the improved mechanical properties, the thermomechanical properties were improved in the sample containing 20 wt% carbon compared to the reference sample with 30 wt% carbon. Difficulties

in homogeneously distributing the nano-scale powders in the refractory matrix as well as the high production cost of these powders were found to be problems [30,31].

In this second part of this work, another way was chosen to lower the carbon content. The starting carbon content was 20 wt%. The aim was to decrease the carbon content from 20 to 15 wt% without downgrading the properties. This work observed a completely new and innovative way of binding matrix manipulation. Another work of the Institute of Ceramics, Glass and Construction Materials showed a possibility to use materials with the ability to emit electrons under reducing conditions (n-type semiconductors) like TiO_2, ZrO_2 as well as P-doped Si (n-Si). This work analysed the influence of these additives on a high basic CaO-MgO-C system. It was found that the transfer of electrons led to an improvement of the novolak resin polymerization and pyrolyzation process. The final result was a partially graphitized glassy carbon lattice and an increased binder carbon yield. Phosphorous-doped silicon was found to be very effective [17]. The doping of Si with P leads to free electrons that are available for charge transfer as schematically shown in Fig. 1.

From the literature it is known that carbon is adsorbed onto the silicon surface and a charge transfer takes place between the adsorbed carbon on the silicon surface and the silicon. Carbon tends to be adsorbed between two silicon surface atoms to saturate its free bonds by means of charge transfer. The Si-C bond length is quite close to the bulk bond length in SiC (1.99 Å). Both carbon and silicon are group IV elements and form alloys and intermixes like SiC [32,33,34]. Thus a charge transfer between the carbon types present in Al_2O_3-C refractories and silicon is likely to be possible. If a charge transfer occurs, an influence on the properties (carbon) is likely to be determinable.

Metallic Si is a common antioxidant in Al_2O_3-C refractories as described above. So it was used in the present work too. Based on the effects described above, the mechanisms and the fact that common silicon is a typical component of the observed system, the strategy was to substitute a small amount of common Si with P-doped n-Si. The use of n-Si was chosen as the only additive to the system to manipulate the binder resin.

A lowering of the carbon content from 30 wt% to 15 wt% means savings of 50 %. This massive lowering means a reduction of CO_2 in case of complete oxidation of this graphite. Per one tonne of produced bricks, this means 150 kg less graphite compared to conventional bricks. This reduction equals 549.6 kg CO_2 (279.92 m³ in the normal state) according to the calculations shown in Table 2.

II. Materials and Methods

As raw materials for the preparation of the investigated Al_2O_3-C compositions (Table 3), a commercially available fine grade of white fused alumina with a maximum grain size of 200 μm, a coarse grade of tabular alumina with a maximum grain size of 600 μm, a fine grade of natural graphite AF (d_{90} = 30 μm), coarse natural flake Graphite NFL (d_{90} = 450 μm) and fine metallic silicon powder of high purity (d_{90} = 50 μm) were used. The observed additive was a phosphorus-doped silicon (d_{90} = 50 μm), which is a donator type (n-type) semi-conductor. The phosphorus-doped silicon had a specific resistance of 1.2 – 1.3 Ohm cm.

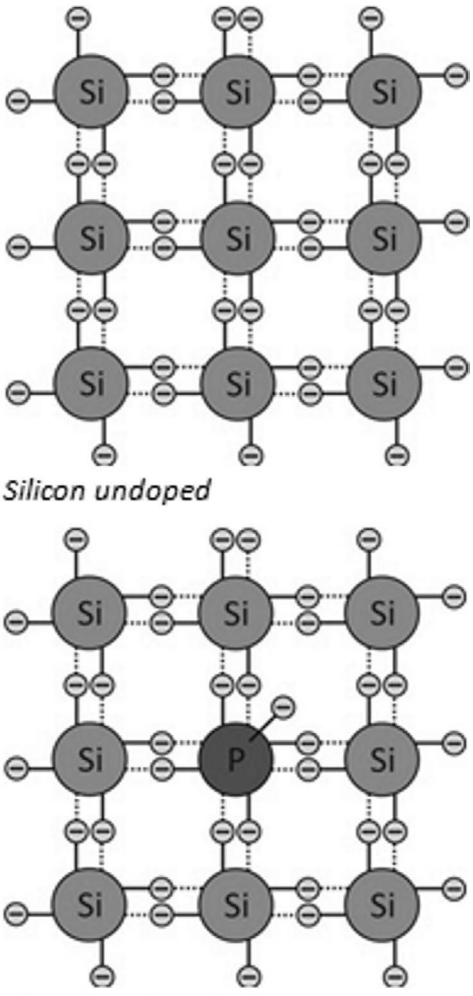

Fig. 1: Model of atomic structure of the used silicon types [34].

Table 2: Calculation of CO_2 formation during carbon oxidation.

$C + O_2 \rightarrow CO_2$ (6)		
M	C	CO_2
n	12.01 g/mol	44.008 g/mol
m	1 g	3.664 g
	150 kg (per 1 ton of produced bricks)	**549.6 kg**
V (DIN 1343) $V=\frac{n \cdot R \cdot T}{p}$ $n=\frac{m}{M}=\frac{549600gmol}{44.008g}$ $=12488.64mol$ R = 8.314472 J/K mol p = 101325 Pa T = 273.15 K		**V = 279.92 m³**

The binder system consisted of a combination of Phenol Novolac resin in liquid (PF 7280 FL 01) and powder form (0235 DP) (Momentive Specialty Chemicals, Germany) with Hexamethylenetetramine (Hexa) as curing agent.

The raw materials and additives were mixed at room temperature in an Eirich compulsory mixer (Maschinenfabrik Gustav Eirich, Germany) according to Table 4, following standard commercial practice. In the first step the Al_2O_3 grains were premixed and then mixed together with the liquid binder component. Afterwards, n-Si powder was added in a single step. In the last step the fines were introduced into the mix and the complete batch was mixed for 5 minutes. After mixing, bar-shaped samples (25 x 25 x 150 mm³) were uniaxially pressed at 100 MPa. The pressed samples were cured in a drying chamber at 200 °C for 2 h. Afterwards the samples were coked at 1000 °C for 5 h in a retort filled with petrol coke. AC20 is the reference sample with a graphite content of 20 wt% based on the work of Roungos *et al.* [30,31] as the starting point for this work as explained before. AC15 is the new reference sample with the target graphite content of 15 wt%.

Table 3: Used raw materials.

raw material	purity	supplier
white fused alumina	> 99.7 wt% Al_2O_3 (max 0.16 wt% Na_2O)	Treibacher Schleifmittel, Austria
tabular alumina	> 99.5 wt% Al_2O_3 (max 0.40 wt% Na_2O)	Almatis, Germany
Graphite AF	> 96 – 97 wt% C	Graphit Kropfmühl, Germany
Graphite NFL	> 94 – 96 wt% C	Graphit Kropfmühl, Germany
metallic Silicon Silgrain	> 99.7 wt% Si	Elkem, Norway
n-Si	> 99.9 wt% Si	Silchem, Germany

The physical and mechanical properties were determined according to EN 933 – 1 open porosity (OP) and bulk density (BD) with water, EN 993 – 6 cold modulus of rupture (CMOR) and in adaption of DIN ENV 843 – 2 static Young's modulus (E). The thermal shock resistance was measured in respect of ENV 993 – 11 with compressed air. The residual CMOR was determined after one (1 TS) and after five (5 TS) thermal shock cycles. The registered strength loss owing to thermal shock gives a first indication of the expected thermomechanical performance of the refractories during their application. The residual carbon content was determined with an elementary analyser vario MICRO cube (Elementar Analysensysteme Hanau GmbH, Germany). The phase composition and the microstructure were investigated with the aid of scanning electron microscope (SEM), energy-dispersive x-ray (EDX) and x-ray diffraction (XRD), respectively.

Table 4: Used compositions.

wt%	AC20	AC20 - Si1	AC15	AC15 - Si1
white fused alumina	29.1		31.2	
tabular alumina	38.9		41.8	
Graphite AF	10		7.5	
Graphite NFL	10		7.5	
liquid resin	2			
powder resin	4			
Hexa	0.6			
n-Si (Phosphor doped)	-	0.5	-	0.5
met. Si	6.0	5.5	6.0	5.5

III. Results and Discussion

(1) Influence of semi-conductive silicon on the physical, mechanical and thermomechanical properties

The addition of 0.5 wt% n-Si led to improved mechanical and physical properties. CMOR was increased by 14 % owing to the n-Si addition in the case of 20 and 15 wt% carbon content as can be seen in Fig. 2. Furthermore, OP decreased and BD increased. The increase of BD and the decrease of OP is related to the evolution of binder carbon yield, which will be discussed later. A very interesting result is the also increased breaking elongation owing to n-Si addition, which is shown in Fig. 3. In the case of both carbon contents, the breaking elongation increased by approximately 8.5 % owing to n-Si addition. The increased breaking elongation is considered to be an indication for a more flexible matrix owing to n-Si addition. All values including the standard deviation are listed in Table 5. A remarkable result is the fact that the CMOR of the sample with 15 wt% graphite containing n-Si is 24 % higher than the CMOR of the reference sample with 20 wt% graphite. This is considered to be an indication that in the system with 15 wt% graphite, the influence of n-Si is stronger.

The evolution of the mechanical properties due to thermal shock cycles shows that in case of a base graphite content of 20 wt% no significant improvement of degradation can be observed. The loss of mechanical strength is with and without n-Si (AC20, AC20-Si1) about 16 % after five thermal shock cycles. For the AC20-Si1 sample the loss is slightly lower than for the AC20 samples. In case of the reference sample with 15 wt% graphite (AC15), the loss of mechanical strength after five thermal shock cycles was much higher with 26 %. This behaviour is expected owing to the reduced graphite content. When n-Si is present in the matrix (AC15-Si1), the evolution of mechanical strength loss showed a completely different behaviour. After one thermal shock cycle the value reached is almost the lowest value. This equals almost the value after five thermal shock

cycles. This is a strong indication of an effective crack network that is going to be formed during the thermal shock cycles.

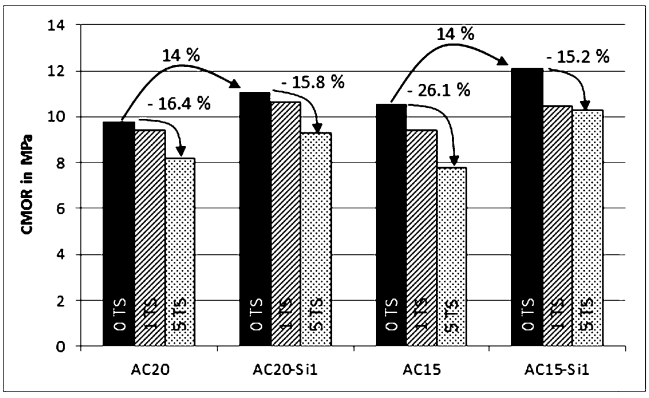

Fig. 2: Mechanical Properties Evolution of tested samples (results after coking – 0 TS, after 1 thermal shock cycle – 1 TS and after 5 thermal shock cycles – 5 TS).

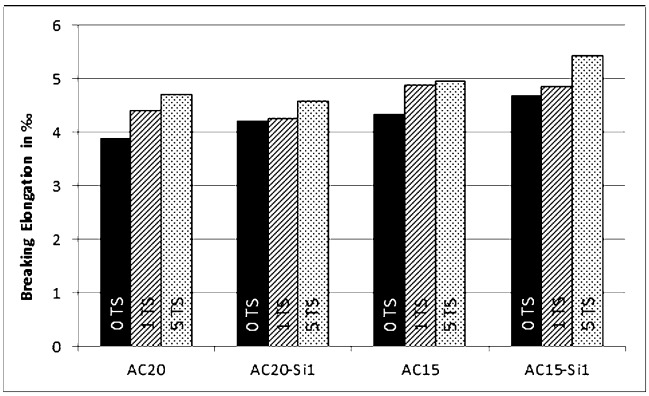

Fig. 3: Breaking elongation of tested samples (results after coking – 0 TS, after 1 thermal shock cycle – 1 TS and after 5 thermal shock cycles – 5 TS)

Cracks are naturally formed during the thermal shock cycles owing to high thermal stresses during the cooling phase caused by the high cooling rate. Cooling leads to tensile stresses on the surface of the sample and if these stresses are above the maximum mechanical strength of the sample cracks will be initiated. The thermal shock coefficient R_1 (Eq. 1) gives a good theoretical basis for the understanding. The most important properties of the samples are the breaking elongation ε (ε = σ/E) and the thermal expansion coefficient α. A large breaking elongation is the expression of a flexible matrix. The larger the breaking elongation and the lower the thermal expansion coefficient, the better the thermal shock resistance [36].

$$R_1 = \sigma_c(i\text{-}v) / E\,\alpha \qquad (7)$$

Sample AC15-Si1 has the largest breaking elongation and shows also the best thermal shock performance. This sample with the lower graphite content of 15 wt% and n-Si shows a better thermal shock performance and better physical and mechanical properties than the reference sample with 20 wt% graphite (AC20).

(2) Influence of semi-conductive silicon on the phase composition and microstructure

A typical XRD scan of the sample investigated after coking at 1000 °C is shown in Fig. 4. The shown x-ray diffractogram of the AC20 sample is representative for the other samples owing to the same determined phases. The spectrum was cut off at 30 000 impulses for better visibility. Table 6 lists the used files and sources for the XRD evaluation. The two main components of the system, Al_2O_3 and graphite, were readily detected as main phases as expected. As secondary phase only β-Al_2O_3 was identified. The reaction of Al_2O_3 and its impurity Na_2O took place in all samples. No Si-based compounds were identified. Only unreacted Si was detected. This is a typical behaviour at a coking temperature of 1000 °C. This was the first indication that the properties evolution of the observed samples was not connected to possible reinforcing reactions of Si with the binding matrix, like the formation of SiC. Hence, no significant additional reactions took place in the sample owing to the use of semi-conductive Si.

Table 5: Physical, mechanical and thermomechanical properties of observed samples (results after coking – 0 TS, after 1 thermal shock cycle – 1 TS and after 5 thermal shock cycles – 5 TS)

	BD	OP	CMOR			E			breaking elongation		
			0 TS	1 TS	5 TS	0 TS	1 TS	5 TS	0 TS	1 TS	5 TS
	[g/cm²]	[%]	[Mpa]	[Mpa]	[Mpa]	[Gpa]	[Gpa]	[Gpa]	[‰]	[‰]	[‰]
R20	2.56 ± 0.02	17.25 ± 0.63	9.78 ± 0.56	9.42 ± 0.55	8.18 ± 0.73	2.515 ± 0.137	2.137 ± 0.199	1.733 ± 0.188	3.89	4.41	4.72
R20-Si1	2.59 ± 0.01	16.21 ± 0.10	11.07 ± 0.30	10.65 ±0.99	9.32 ± 0.69	2.624 ± 0.087	2.497 ± 0.178	2.027 ± 0.163	4.22	4.27	4.60
R15	2.60 ± 0.00	18.68 ± 0.25	10.53 ± 0.31	9.43 ± 0.89	7.78 ± 0.76	2.434 ± 0.211	1.928 ± 0.202	1.565 ± 0.111	4.32	4.89	4.97
R15-Si1	2.64 ± 0.01	17.11 ± 0.29	12.11 ± 2.05	10.46 ± 1.13	10.27 ± 1.45	2.585 ± 0.169	2.148 ± 0.215	1.891 ± 0.183	4.69	4.87	5.43

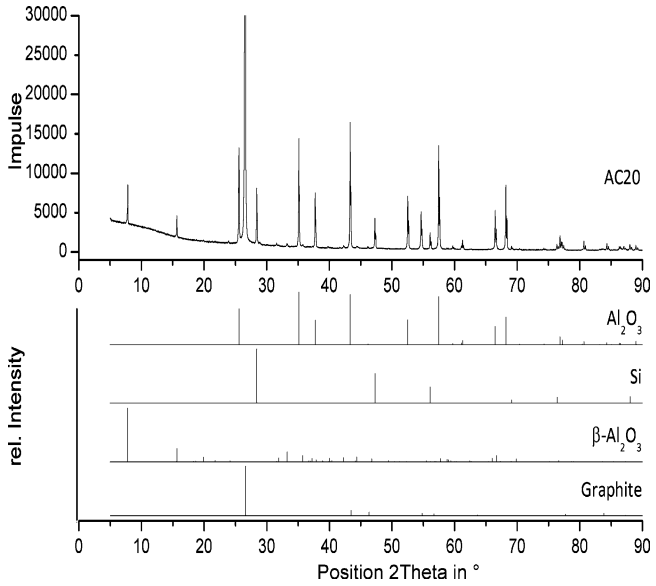

Fig. 4: XRD pattern of AC20 sample with the relative intensity patterns of the identified phases.

Table 6: Used XRD raw files.

Phase	PDF-Number
Al_2O_3	01-081-1667
Si	00-027-1402
β-Al_2O_3	01-079-2288
Graphite	01-075-2078

The data from the XRD evaluation was confirmed with SEM micrographs. As can be seen in Fig. 5 to Fig. 8, no newly formed phases were identified in the matrix of the samples. All micrographs showed the typical highly jointed structure consisting of Al_2O_3 grains, graphite flakes, and Si spheres. No whisker structures were identified, as was not to be expected otherwise in respect of the coking temperature of 1000 °C [30,31].

Both reference samples, with 20 and 15 wt% graphite, have a binder carbon yield of approximately 35 wt%. In both cases the addition of n-Si leads to increased binder carbon yield. As can be seen in Fig. 9, the influence of n-Si addition on the binder carbon yield is more effective in the Al_2O_3-C system with the lower graphite content. In case of a graphite content of 20 wt%, the binder carbon yield has been increased from 35 to approximately 45 wt%. In the system with 15 wt% graphite the binder carbon yield has been increased from 35 to approximately 60 wt%. The smaller influence of n-Si on the system with the higher graphite content is related to the formation of CO gas during the coking procedure, which limits the activating influence of n-Si. The binder carbon yield was calculated according to Eq. 2 from the determined carbon content of the samples. All values including the standard deviation are listed in Table 7. The increase of binder carbon yield leads to fewer defects in the matrix and thus a lower OP and a higher BD.

$$\text{Binder Carbon Yield}(\%) = 100\% \cdot \frac{\text{C.Y.}_{(\text{Total})} - \text{C.Y.}_{(\text{Graphite AF})} - \text{C.Y.}_{(\text{Graphite NFL})}}{\text{Initial Binder Content}} \quad (8)$$

C.Y. = Carbon Yield

$$\text{C.Y.}_{(\text{Graphite AF})} = 0.96 \cdot x_{\text{Graphite AF}}$$

$$\text{C.Y.}_{(\text{Graphite NFL})} = 0.96 \cdot x_{\text{Graphite NFL}}$$

Initital Binder Content = 6 wt%

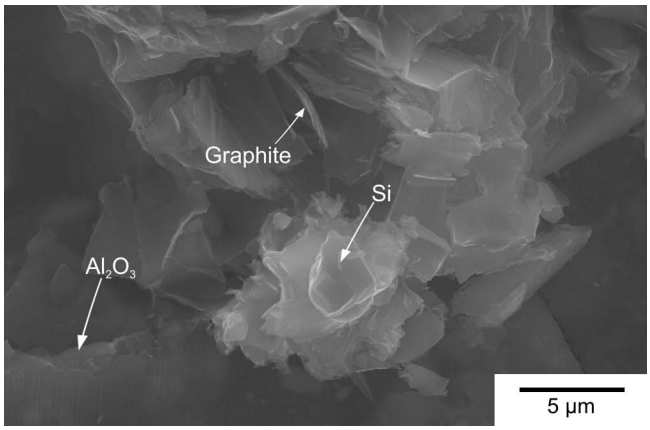

Fig. 5: Fracture surface of Al_2O_3-C sample with 15 wt% C (3000x).

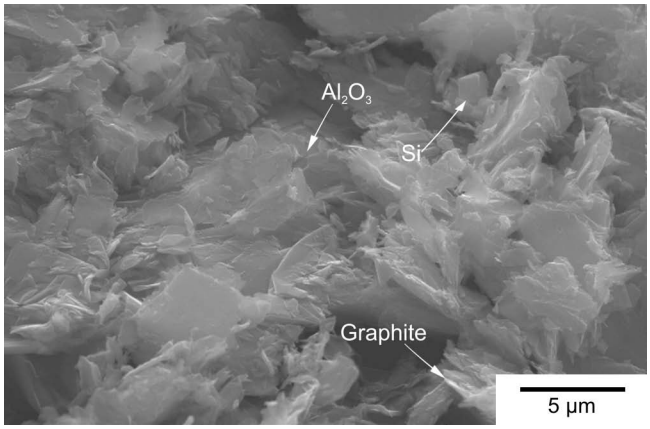

Fig. 6: Fracture surface of Al_2O_3-C sample with 15 wt% C and 0.5 wt% n-Si (3000x).

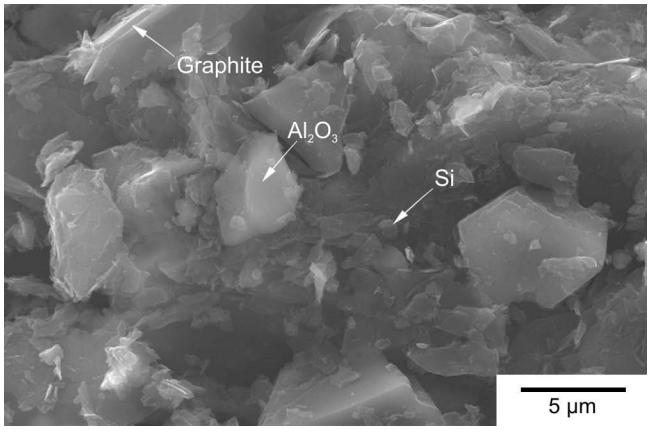

Fig. 7: Fracture surface of Al_2O_3-C sample with 20 wt% C (3000x).

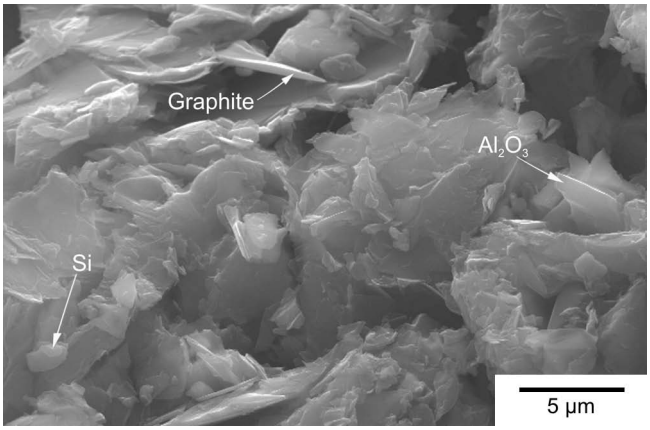

Fig. 8: Fracture surface of Al_2O_3-C sample with 20 wt% C and 0.5 wt% n-Si (3000x).

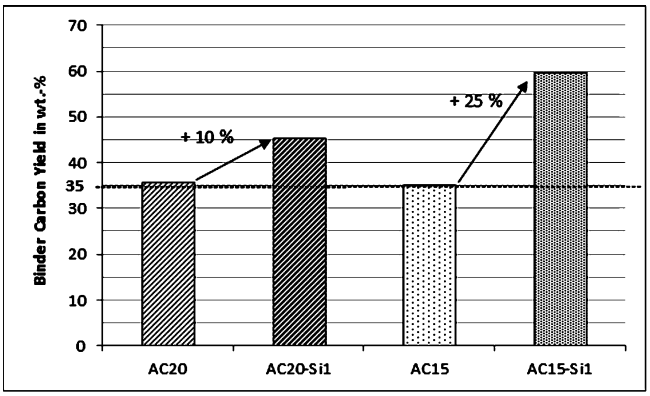

Fig. 9: Binder carbon yield of the observed samples.

Table 7: Carbon content and binder carbon yield of the investigated samples.

	Carbon Content	Binder Carbon Yield
	[wt%]	[wt%]
R20	21.35 ± 0.11	35.8 ± 1.8
R20-Si1	21.92 ± 0.11	45.3 ± 1.9
R15	16.51 ± 0.08	35.2 ± 1.4
R15-Si1	17.98 ± 0.06	59.7 ± 1.1

(a) ***Mechanism of n-Si influence***

The positive influence of n-Si on the properties evolution of Al_2O_3-C refractories was shown impressively in Sections 3.1 and 3.2. But phase analysis showed no reactions between added Si or n-Si with the surrounding carbon matrix or with Al_2O_3. Thus the positive influence is considered to be related to a charge transfer between n-Si and the binder matrix. This effect had been shown before with the addition of n-Si into a CaO-MgO-C refractory system [17]. The added n-Si was of the same specifications as the n-Si used in the present work. An electron transfer occurred, which led to a stabilized resite lattice and further initiated graphitization.

The structure of novolak is a planar hexagon with carbon atoms on the edges. Hydrogen atoms are bonded with these carbon atoms. Furthermore, an OH-group and a CH_2 group are bonded with the planar hexagon (Fig. 10) [9]. Dehydration of this structure while the bonds are saturated leads to a simplified graphite crystal seed.

During the pyrolysis process, novolak molecules are dehydrated. The electrons transferred from n-Si saturate the bonds and lead to graphitized zones in the dehydrating resite lattice during the pyrolysis process as shown in Fig. 11. A short range order of graphitized areas is formed as explained above. These additional graphitic areas work as seeds for on-going graphitization as a result of the occurring electron charge. These partially graphitized zones in the glassy carbon lattice transform the stiff and brittle structure into a more flexible structure on account of the special properties of graphite. In parallel direction to the layers, graphite is bonded by a weak van der Waals force. So it is possible to disarrange the layers against each other easily [2]. Thus graphitization of the bonding matrix leads to a stronger flexibility, which can be seen in the increasing breaking elongation of the samples containing n-Si. The improved mechanical properties are related to improved polymerization of the resite lattice, as observed previously [17].Graphitized zones deliver additional areas with graphite-like properties, which leads to the improved properties of the compound material. Furthermore, n-Si leads to higher binder carbon yield. Owing to the stabilized resite lattice structure, the loss of carbon is lower than in the unstabilized lattice. So we can talk about two related mechanisms that improve the properties of the binding carbon matrix and further the properties of the carbon-bonded composite material.

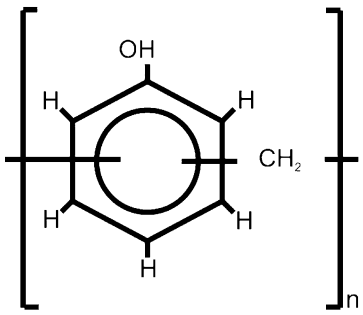

Fig. 10: Simplified structure of a novolak molecule[9].

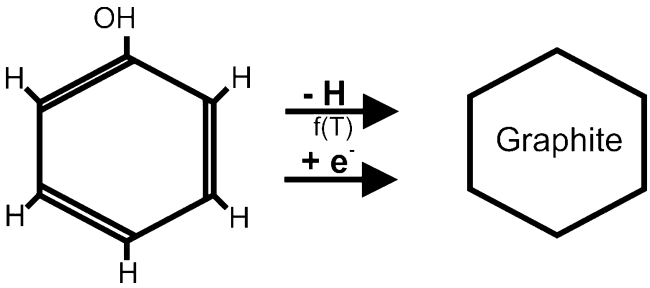

Fig. 11: Scheme of electron transfer effect on graphitization of novolak.

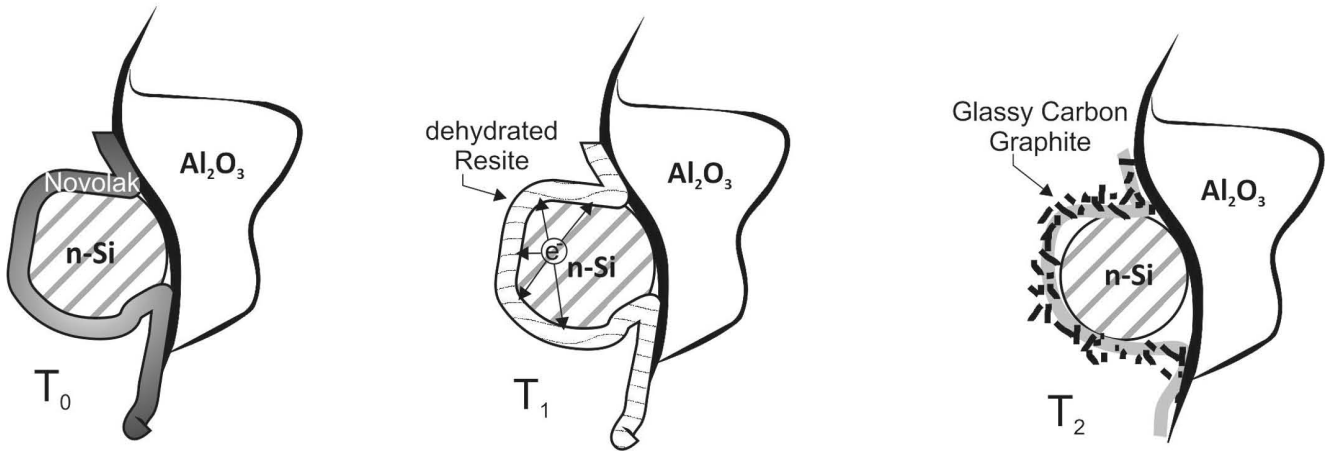

Fig. 12: Schematic draft of the n-Si influence on the phenol-novolak partial graphitization in Al_2O_3-C refractories (T_0 – situation before firing; T_1 – above 300 °C – 400 °C novolak is transformed into resite lattice, which is dehydrated with increasing temperatures, from n-Si electrons are delivered to the dehydrated resite, these electrons stabilize the bonding between carbon atoms in the residual planar hexagon from initial novolak molecule and support graphitization ; T_2 – above 500 °C – 600 °C n-Si surrounded by glassy carbon and graphitized glassy carbon)

IV. Conclusions

In this work it was possible to reduce the graphite content of Al_2O_3-C refractories from 20 to 15 wt% while improving their properties. The addition of n-Si to the Al_2O_3-C system led to improved physical, mechanical as well as thermomechanical properties thanks to the stabilizing mechanism of the glassy carbon lattice.

Phosphorus-doped Si (n-type semiconductor) showed the ability to activate and assist glassy carbon graphitization by emitting electrons to the glassy carbon structure and thus stabilizing the turbostratic graphitic structure to graphite under reducing conditions. These conditions are predominant inside carbon-bonded refractories. During carbonization of the binder resin, the resite molecules are dehydrated and form the turbostratic graphitic structure. Donated electrons stabilize the bonding in the disordered structure and force the graphite formation, which leads to a reinforced binder matrix. This mechanism reinforced the carbon-binding matrix, leading to improved mechanical and physical properties. It is a new and innovative way to manipulate the binding glassy carbon lattice. Furthermore, the interaction between the electron-emitting additive and the binder resin increases the carbon yield (from 35 to 60 wt% binder carbon yield in the case of AC15-Si1) of the binder resin. These interactions reduce emissions and lead to economic utilization of assigned resources.

Fig. 12 shows a schematic draft of the model of the n-Si influence on the phenol-novolak partial graphitization in Al_2O_3-C refractories.

The modified partially graphitized glassy carbon lattice made it possible to reduce the graphite content. Consequently, emissions can be reduced as well as emissions from the binder during pyrolysis process. In this context it is very important that the physical, mechanical and thermomechanical properties are not downgraded. On the contrary, the properties are improved. This is an important step towards environmentally friendly refractories. In view of the low amount of n-Si used, that is 0.5 wt%, it seems an economical approach to improve the properties of Al_2O_3-C refractories in application.

Accordingly, it was possible to reduce the graphite content from 20 to 15 wt% by using an electron-emitting additive (n-type semi-conductor) in the binder system. Furthermore, the aim of improving the physical, mechanical and thermomechanical properties was achieved. By increasing the breaking elongation and the mechanical strength, the thermal shock performance was improved.

This work as the second part in a larger context reached the target carbon content of 15 wt%. The first part of this work reached a carbon content reduction from 30 to 20 wt%. So it was possible to achieve a carbon content reduction of at least 50 %, which means theoretical savings of 549.6 kg CO_2 (279.92 m³ at normal state) per tonne of produced Al_2O_3-C refractories.

Acknowledgements

The authors thank the GRF (German Research Foundation) for funding this work within the Priority Program 1418. The work was conducted at the Institute of Ceramics, Glass and Construction Materials.

References

1 Pierson, H.O.: Handbook of carbon, graphite, diamond and fullerenes – properties, processing and applications. Noyes Publications, Park Ridge, New Jersey, 1993.

2 Krüger, A.: New carbon materials – an introduction, (in German), 1st edition. B.G. Teubner Verlag, Wiesbaden, 2007.

3 Salmang, H., Scholze, H., Telle, R.: Ceramics, (in German), 7th edition. Springer-Verlag, Berlin, Heidelberg, 2007.

4 Richmond, C.: Doloma Refractories. In: Refractories Handbook. (Editor Schacht, C.A.) Marcel Dekker Inc., New York-Basel, 2004.

5 Pocket Manual Refractory Materials. (Editor Routschka, G.) 3rd edition. Vulkan-Verlag Essen, 2008.

6 Trojer, F., Obst, K.H., Münchberg, W.: Mineralogy of basic refractory products, (in German), Springer Verlag, Vienna-New York, 1981.

7 Naghibi, S., Nemati, Z.A., Faghihi Sani, M.A., Paidar, H.: The effects of graphite and resin contents on the properties of doloma-graphite refractories. Proceedings of the Unified International Technical Conference on Refractories, Orlando, USA, 2005.

[8] Barin, I., Knacke, O., Kubaschewski, O.: Thermochemical properties of inorganic substances. Springer Verlag, Berlin-Heidelberg-New York, 1973.

[9] Gardziella, A.: Chemistry and physics of duroplastic resins in plastics handbook vol.10 duroplastics, (in German), Editors: Becker, G.W., Braun, D., Woebcken, W., Carl HanserVerlag, Munich, Vienna, 1988.

[10] Lewis, I.C.: Chemistry of carbonization, *Carbon*, **20**, [6], 519 – 529, (1982),

[11] Guan, G., Kusakabe, K., Ozono, H., Taneda, M., Uehara, M., Maeda, H.: Preparation of carbon microparticle assemblies from phenolic resin using an inverse opal templating method, *J. Mater. Sci.*, **42**, 10196 – 10202, (2007).

[12] Yamada, S., Sato, H., Ishii, T.: Properties and application of glassy carbon (in German), *Carbon*, **2**, 253 – 260, (1964).

[13] Lersmacher, B., Lydtin, H., Knippenberg, W.F.: Glassy carbon (in German), *Chem.Ing. Tech.*, **42**, 659 – 669, (1970).

[14] Fitzer, E.: Thermal degradation of polymers to elementary carbon – a path to the materials of the future (in German), *Angew. Chem.*, **92**, 375 – 386, (1980).

[15] Fitzer, E., Weissweiler, W.: Kinetics of catalytic graphitization with iron metals, (in German), *Chem.Ing. Tech.*, **44**, 972 – 979, (1972).

[16] Bartha, P., Jansen, H., Grosse Daldrup, H.: Composition, application and process for the production of carbon-containing shaped refractories with enhanced oxidation behaviour, (in German). European Patent EP 1 280 743 B1, (2004).

[17] Stein, V.: Contribution to the characteristic improvement of carbon bonded doloma refractories by addition of functional ceramic materials, Freiberger Forschungsheft, Reihe A 905, (2011).

[18] Stein, V., Aneziris, C.G., Guéguen, E.: New approach for the application of functional ceramic material in carbon bonded doloma refractories to reduce emissions, *Adv. Eng. Mater.*, **13**, 1135 – 1141, (2011).

[19] Stein, V., Aneziris, C.G., Guéguen, E., Hill, K.: A prospective way to reduce emissions in secondary steel making metallurgy by application of functionalised doloma carbon refractories, *Int. J. Appl. Cer. Tech.*, **9**, 615 – 624, (2012).

[20] Kyoto Protocol, Third International Conference of the Parties, Kyoto, Japan, December 11, 1997

[21] Bundes-Immissionsschutzgesetz BImSchG: mit Durchführungsverordnungen, Emissionshandelsrecht, TA Luft und TA Lärm [Germany's Federal Ambient Pollution Control Act], 10th edition, Deutscher Taschenbuch Verlag, 2010.

[22] Khezrabadi, M.N., Javadpour, J., Rezaie, H.R., Naghizadeh, R.: The effect of additives on the properties and microstructures of Al_2O_3-C refractories, *J. Mater. Sci.,* **41**, 3027 – 3032, (2006)

[23] Yamaguchi, A.: Self-repairing function in the carbon-containing refractory, *Int. J. Appl. Cer. Tech*., **4**, 490 – 495, (2007)

[24] Sunayama, H., Kawahara, M., Mitsuo, T., Sumitomo K.: The effect of B_4C addition on the oxidation resistance of Al_2O_3-C and Al_2O_3-SiC-C refractories, Proceedings of the Unified International Technical Conference on Refractories, New Orleans, USA, 1997.

[25] Zhang, S., Yamaguchi, A.: A comparison of Al, Si and Al_4SiC_4 added to Al_2O_3-C refractories, Proceedings of the Unified International Technical Conference on Refractories, New Orleans, USA, 1997.

[26] Vieira, W. Jr., Rand, B.: The nature of the bond in silicon-containing alumina-carbon refractory composites – Part I., Proceedings of the Unified International Technical Conference on Refractories, New Orleans, USA, 1997.

[27] Zhang, S.: Next generation carbon-containing refractory composites, *Adv. Sci. Tech.* **45**, 2246 – 2253, (2006).

[28] Luhrsen, E., Ott, A.: Immersion nozzles for metal melts. U.S. Patent 5,171,495, 15. (1992).

[29] Wang, T., Yamaguchi, A.: Antioxidation behavior and effect of $Al_8B_4C_7$ added to carbon-containing refractories, *J. Ceram. Soc. Japan*, **108**, 818 – 822, (2000).

[30] Roungos, V., Aneziris, C.G.: Improved thermal shock performance of Al_2O_3-C refractories due to nanoscaled additives, *Cer. Int.*, **38**, 919 – 927, (2012).

[31] Roungos, V., Aneziris, C.G., Berek, H.: Novel Al_2O_3-C refractories with less residual carbon due to nanoscaled additives for continuous steel casting applications, *Adv. Eng. Mat.*, **15**, 255 – 264, (2012).

[32] Khoo, G.S., Ong, C.K.: The interactions of metallic and semiconducting adsorbates with Si(100), *J. Phys.: Condens. Mat.*, **6**, 8141 – 8148, (1994).

[33] Hayashi, Y., Ishikawa, S., Soga, T., Umeno, M., Jimbo, T.: Photovoltaic characteristics of boron-doped hydrogenated amorphous carbon on n-si substrate prepared by r.f. plasma-enhanced CVD used trimethylboron, *Diam. Relat. Mater.*, **12**, 687 – 690, (2003).

[34] Xue, Q.Z., Zhang, X.: Anomalous electrical transport properties of amorphous carbon films on si substrates, *Carbon*, **43**, 760 – 764, (2005).

[35] Riedel, H.: General and inorganic chemistry, (in German), 8th edition. Walter de Gruyter, Berlin, New York, 2004

[36] Kingery, W.D.: Factors affecting thermal stress resistance of ceramic materials, *J. Am. Ceram. Soc.*, **38**, 3 – 15, (1955).